

INVESTIGATION OF ELECTRONIC, STRUCTURAL AND MECHANICAL PROPERTIES OF $\text{FeMnP}_{1-x}\text{A}_x$ ($\text{A}_x=\text{Si, Ga, Ge}$; $x=0.33$ and $1-x = 0.67$) AS A POTENTIAL MAGNETOCALORIC REFRIGERANT ALLOY.

Gabriel Chirchir Kipkemei.
gabrielchirchir@gmail.com

1. Abstract or Introduction

Exhaustive *ab initio* calculations within the GGA are carried out to identify possible Fe_2P -type giant magnetocaloric $\text{FeMnP}_{1-x}\text{Si}_x$ alloys. The calculated elastic constants confirm the mechanical stability for the Fe_2P -type hexagonal $\text{FeMnP}_{1-x}\text{Si}_x$ alloys in both ferromagnetic (FM) and antiferromagnetic (AFM) phases. The predicted elastic properties for $\text{FeMnP}_{0.67}\text{Si}_{0.33}$ are close to those obtained for $\text{FeMnP}_{0.67}\text{Ga}_{0.33}$ and $\text{FeMnP}_{0.67}\text{Ge}_{0.33}$ using the same calculation scheme. The electronic density of states confirms that the $\text{FeMnP}_{0.67}\text{Si}_{0.33}$ alloys have similar electronic structures to those of $\text{FeMnP}_{0.67}\text{Ga}_{0.33}$ and $\text{FeMnP}_{0.67}\text{Ge}_{0.33}$. The results predict that $\text{FeMnP}_{0.67}\text{Ga}_{0.33}$ is the best candidate refrigerant for room temperature magnetic refrigeration because of its high ductility during phase transition from FM to AFM phase. On substituting Mn element in the 3g site with the Re element, ductility was acquired in all the three alloys that is $\text{FeMn}_{1-x}\text{Re}_x\text{P}_{1-x}\text{A}_x$ ($\text{A}=\text{Si, Ga, Ge}$) alloys, making the alloys best refrigerants at room temperature

2. Computational Details

Investigation of the structural, electronic and mechanical effects on $\text{FeMnP}_{1-x}(\text{Si, Ga, Ge})_x$ and $\text{FeMn}_x\text{Re}_{1-x}\text{P}_{1-x}(\text{Si, Ga, Ge})_x$ ($x = 0.33$ and $1 - x = 0.67$) were calculated under the generalized gradient approximation (GGA) using the DFT method. The DFT method was implemented in the QE code. The Perdew Burke Ernzerhof (PBE) pseudo-potentials type were chosen as exchange correlation functional during the calculations. The kinetic energy cut off parameter for the unit cell structure was optimized at 360 Ry. The relaxed input file used supported Monkhorst-Pack k-points mesh of $3 \times 3 \times 5$ calculations on the FM hexagonal phase. In the reciprocal space, fitting of $3 \times 3 \times 2$ k-points mesh was used to sampled Brillouin zone integration in the AFM phase. The conjugate gradient parameter was set in the optimized unit cell structure and implemented in the Thermo_pw code to calculate elastic properties. The electronic DOS calculations for $\text{FeMnP}_{1-x}(\text{Si, Ga, Ge})_x$ and $\text{FeMn}_x\text{Re}_{1-x}\text{P}_{1-x}(\text{Si, Ga, Ge})_x$ at ($x = 0.33$ and $1 - x = 0.67$) alloys were carried out at the $\Gamma, \text{H, K, L, M, } \Gamma$ symmetry lines. The $\Gamma, \text{H, K, L, M, } \Gamma$ symmetry path was generated using the google seek path package.

3. Results

3.1 Structural properties

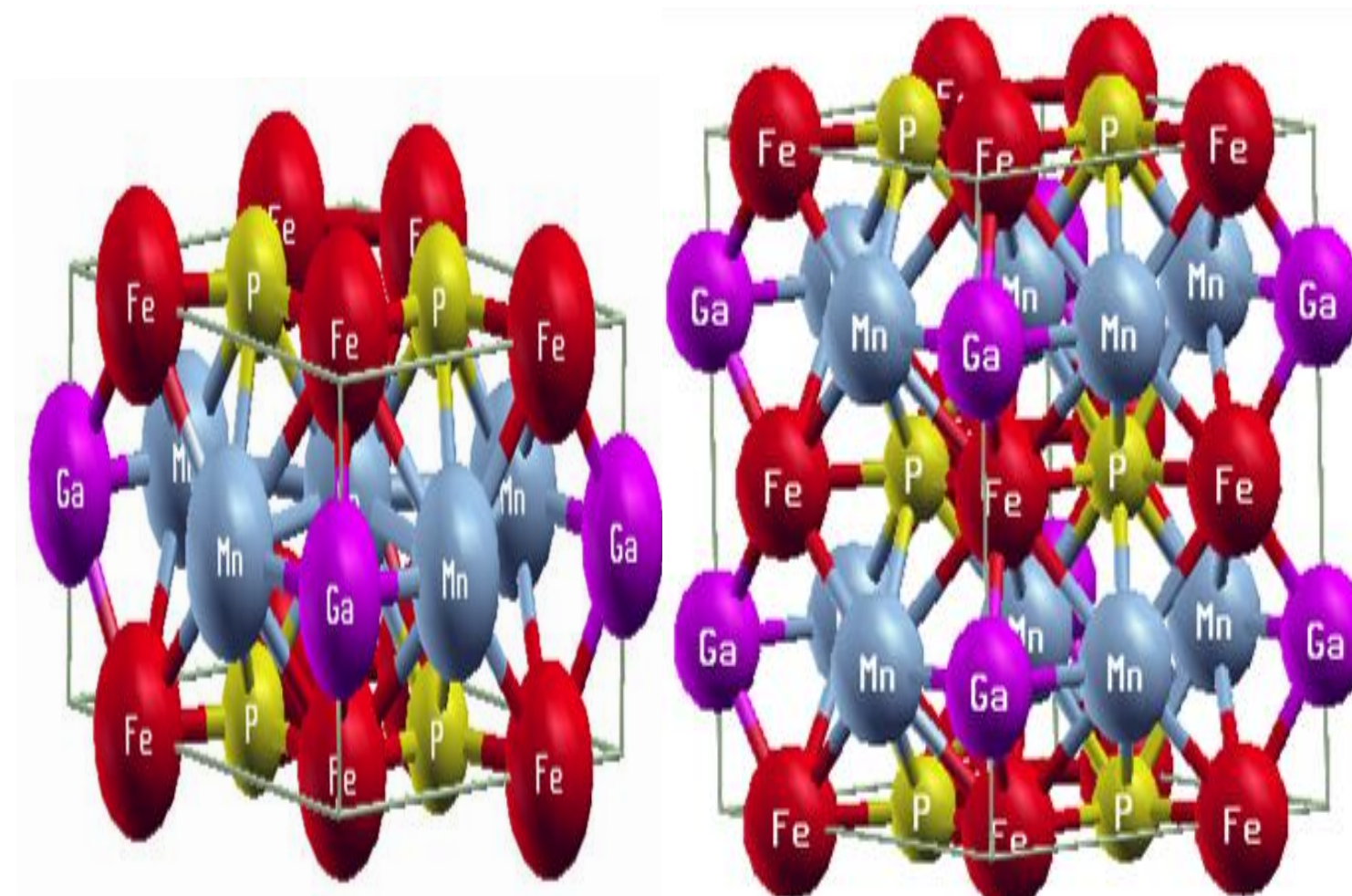


Figure 1: Unit cell structure for $\text{FeMnP}_{1-x}\text{Ga}_x$ alloy

Figure 2: Supercell structure for $\text{FeMnP}_{1-x}\text{Ga}_x$ alloy

Table 1: Calculated DFT-(PBE-GGA) lattice parameters for the $\text{FeMn}_{1-x}\text{Re}_x\text{P}_{1-x}\text{A}_x$ Alloy.

$\text{FeMn}_{1-x}\text{Re}_x\text{P}_{1-x}\text{A}_x$ ($\text{A}_x=\text{Si, Ga, Ge}$) Lattice parameters			
	$a(\text{\AA})$	$c(\text{\AA})$	$V(\text{\AA}^3)$
FM			
Si	5.8860	3.6642	106.4440
Ga	6.14290	3.35209	110.2272
Ge	5.9722	3.7301	109.8805
AFM			
Si	5.8471	3.6600	105.8080
Ga	5.9194	3.7641	109.8673
Ge	6.1507	3.4811	113.9768

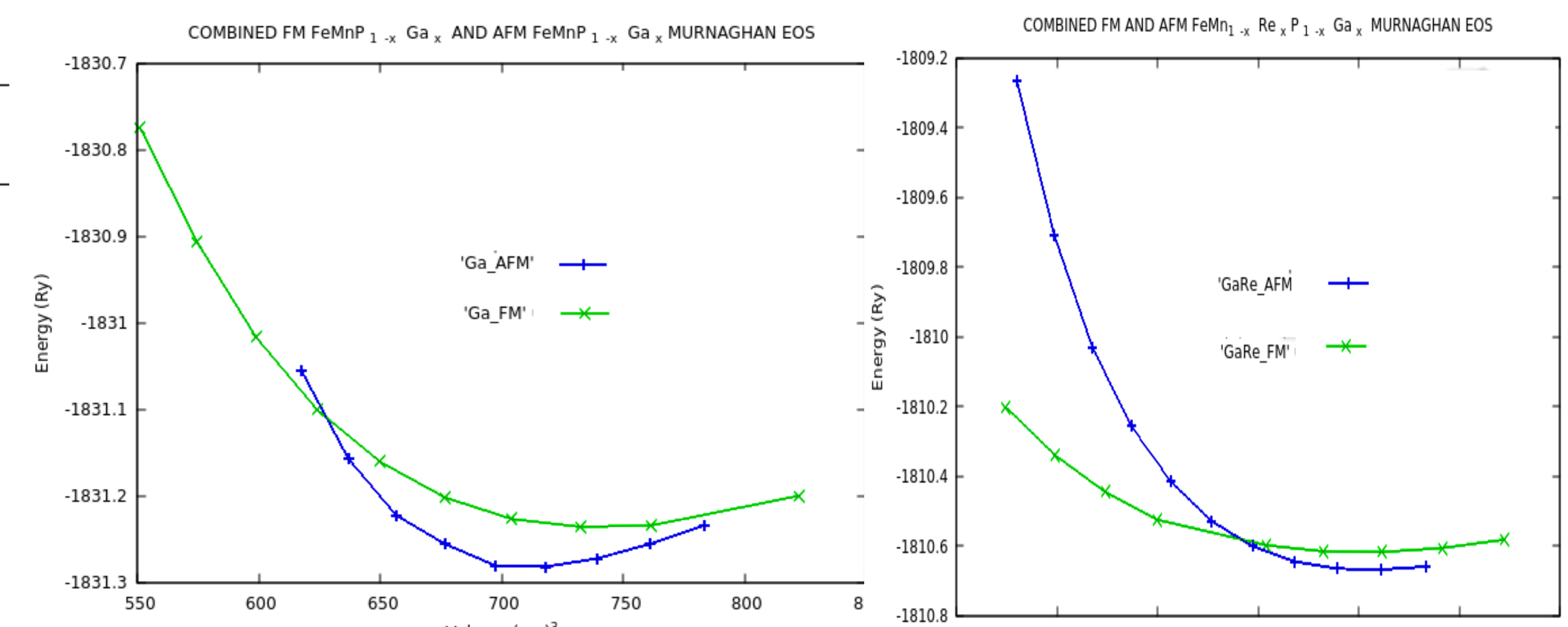


Figure 3: Murnaghan EOS for combined FM and AFM $\text{FeMnP}_{1-x}\text{Ga}_x$ alloy

Figure 4: Murnaghan EoS for combined FM and AFM $\text{FeMn}_{1-x}\text{Re}_x\text{P}_{1-x}\text{Ga}_x$ alloy

3.2 Electronic properties

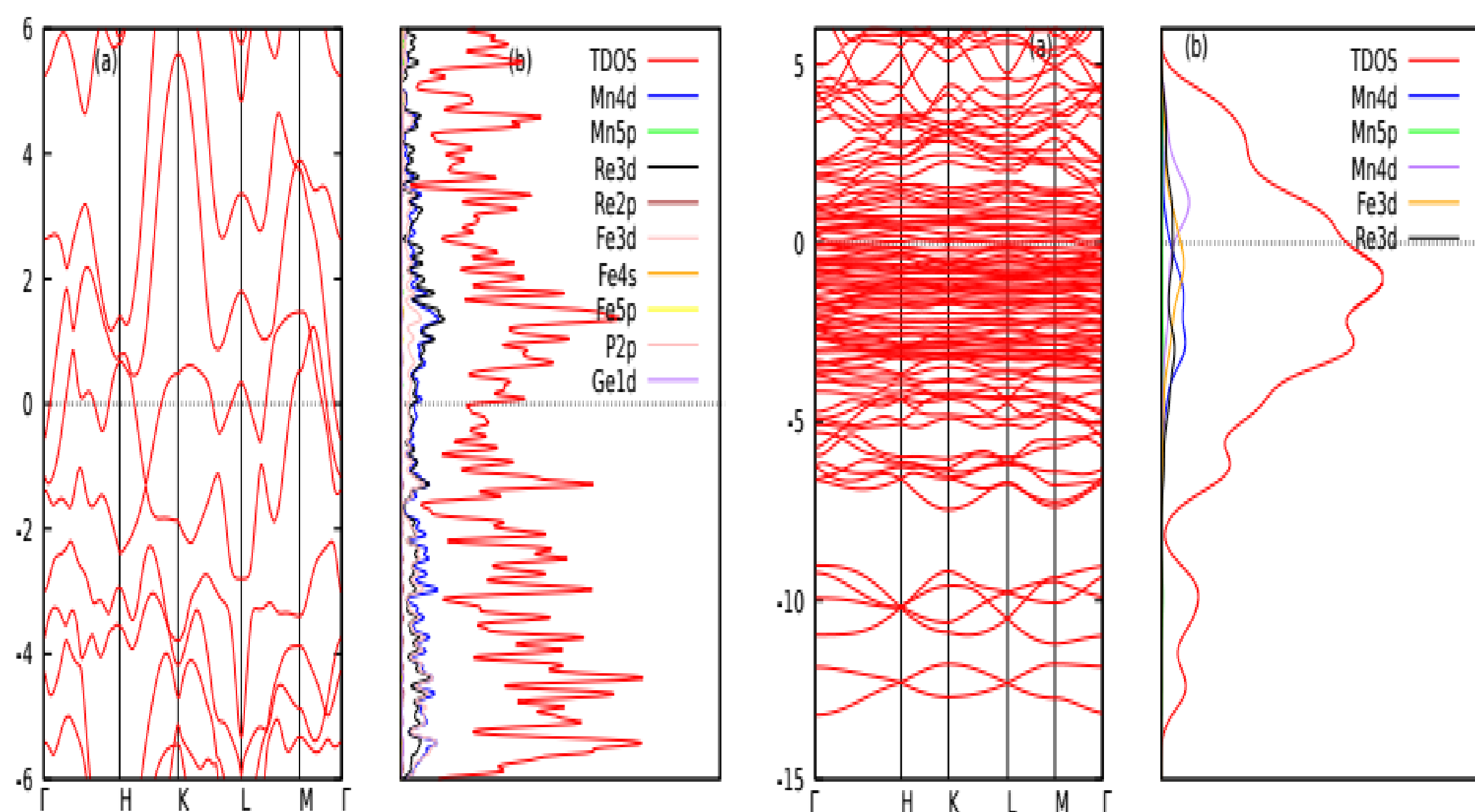


Figure 5: PDOS for FM $\text{FeMn}_{1-x}\text{Re}_x\text{P}_{1-x}\text{Ga}_x$ alloy

Figure 6: PDOS for AFM $\text{FeMn}_{1-x}\text{Re}_x\text{P}_{1-x}\text{Ga}_x$ alloy

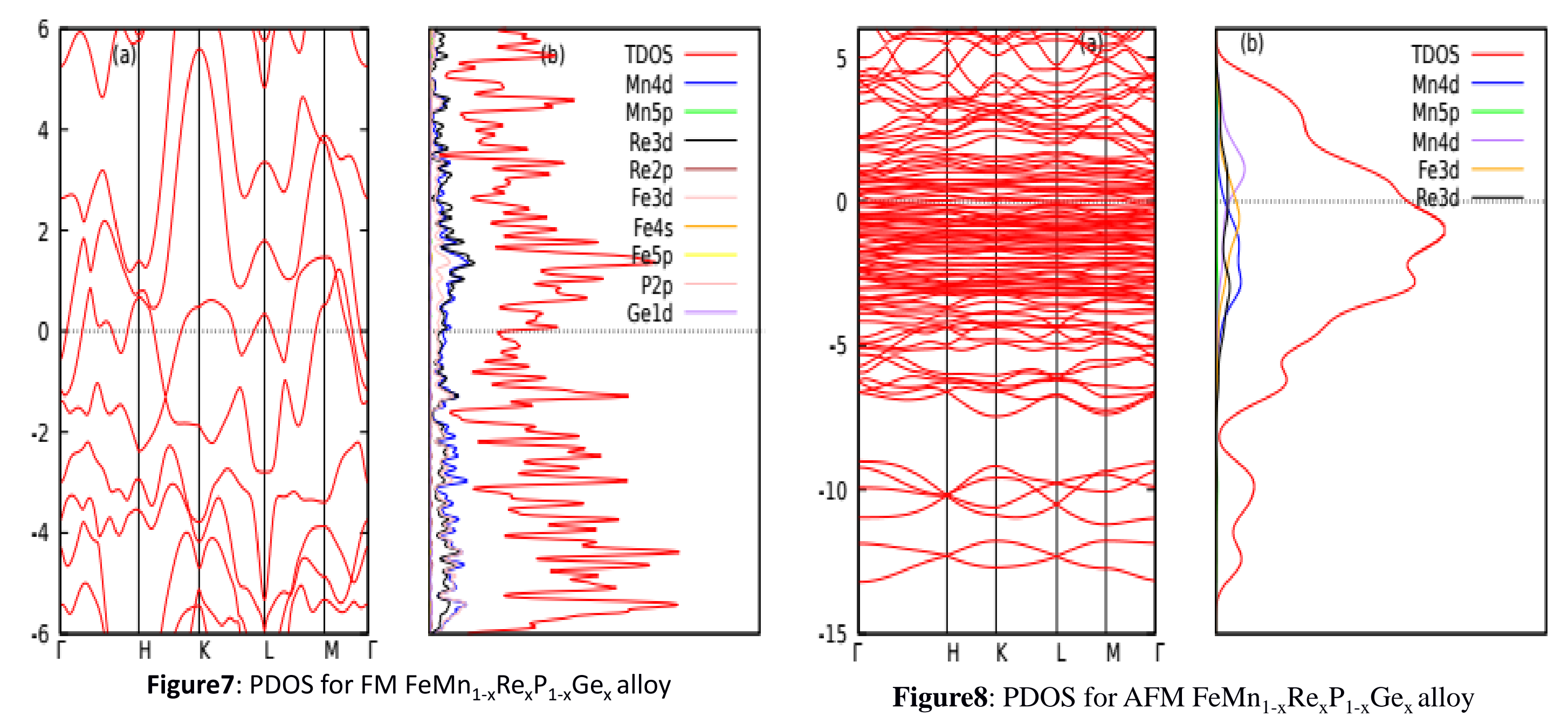


Figure 7: PDOS for FM $\text{FeMn}_{1-x}\text{Re}_x\text{P}_{1-x}\text{Ge}_x$ alloy

Figure 8: PDOS for AFM $\text{FeMn}_{1-x}\text{Re}_x\text{P}_{1-x}\text{Ge}_x$ alloy

3.3 Elastic properties

Table 2: The $\text{FeMnP}_{1-x}\text{A}_x$ alloys Bulk modulus (B) and shear modulus (G) in GPa under the Voigt, Reuss, and Hill averaging schemes, Young's modulus (E) in GPa, Poisson's ratio (n) and Debye temperature θ_D (K) for the $\text{FeMnP}_{1-x}\text{A}_x$ alloy.

		B_V	B_R	G_V	G_R	G_H	B_H	B_H/G_H	E	n	θ_D (K)	
		(GPa)										
$\text{FeMnP}_{1-x}\text{A}_x$ ($\text{A}_x=\text{Si, Ga, Ge}$) $x=0.33$												
Si	FM	187.1	187.0	85.5	70.6	78.1	187.1	2.39	205.5	0.31546	361.648	
	AFM	175.9	174.8	105.8	106.3	106.3	175.4	1.65	265.3	0.24785	579.297	
Ga	FM	182.7	182.7	80.4	44.2	62.3	182.7	2.93	166.6	0.33636	428.113	
	AFM	153.1	153.1	84.0	82.0	83.0	153.1	1.84	210.9	0.27042	493.565	
Ge	FM	155.9	154.9	74.4	67.1	70.8	155.4	2.19	184.3	0.30190	331.5	
	AFM	143.2	143.3	85.7	84.3	85.0	143.3	1.68	213.0	0.25220	496.9	

Table 3: $\text{FeMn}_{1-x}\text{Re}_x\text{P}_{1-x}\text{A}_x$ ($\text{A}_x=\text{Si, Ga, Ge}$) alloys Bulk modulus (B) and shear modulus (G) in GPa under the Voigt, Reuss, and Hill averaging schemes, Young's modulus (E) in GPa, Poisson's ratio (n) and Debye temperature θ_D (K) for the $\text{FeMn}_{1-x}\text{A}_x$ ($\text{A}_x=\text{Si, Ga, Ge}$) alloy.

		B_V	B_R	G_V	G_R	G_H	B_H	B_H/G_H	E	n	θ_D (K)	
		(GPa)										
$\text{FeMn}_{1-x}\text{Re}_x\text{P}_{1-x}\text{A}_x$ ($x=0.33$)												
Si	FM	100.9	88.5	67.9	45.8	56.8	94.7	1.67	141.8	0.24702	373.994	
	AFM	181.0	174.0	77.4	74.3	75.8	175.6	2.32	99.2	0.31299	420.227	
Ga	FM	124.0	61.3	54.9	99.2	77.1	368.5	4.779	213.1	0.38174	132.635	
	AFM	153.1	153.1	84.0	82.0	83.0	153.1	1.84	210.9	0.27042	341.577	
Ge	FM	134.6	62.9	38.2	61.5	49.8	98.8	1.984	127.8	0.28090	342.456	
	AFM	188.6	181.5	73.0	22.1	47.6	185.1	3.88	128.9	0.35492	341.577	

Table 4: Elastic constants for the $\text{FeMnP}_{1-x}\text{A}_x$ ($\text{A}_x=\text{Si, Ga, Ge}$) alloys.

		C_{11}	C_{12}	C_{13}	C_{33}	C_{44}	C_{66} (GPa)
$x=0.33$							
Si	FM	290.2	110.6	163.7	227.7	107.3	89.7
	AFM	331.6	107.0	118.8	273.3	112.6	111.3
Ga	FM	265.6	109.5	173.2	201.5	116.0	78.0
	AFM	250.3	97.8	108.2	243.8	99.7	76.6
Ge	FM	237.3	86.2	133.7	220.9	91.4	75.5
	AFM	244.6	82.0	100.8	243.2	98.4	83.2

4. Conclusion

The optimized lattice parameters were in good agreement with the experimental and literature values. The electronic calculations predict $\text{FeMnP}_{1-x}\text{A}_x$ alloys are metallic in both FM and AFM phase since all three alloys exhibits no bad gap. It was also shown that the substitution of Mn element in the 3g site with the Re element gives ductility across the three alloys in the $\text{FeMn}_{1-x}\text{Re}_x\text{P}_{1-x}\text{A}_x$ alloys.

5. References

- [1] Kavita, S., Anusha, G., Bhatt, P., Suresh, V., Vijay, R., Sethupathi, K., & Gopalan, R. (2020). On the giant magnetocaloric and mechanical properties of Mn-Fe-P-Si-Ge alloy. *Journal of Alloys and Compounds*. **817**, 153232-153238.
- [2] Höglin, V., Cedervall, J., Andersson, M. S., Sarkar, T., Hudl, M., Nordblad, P., & Sahlberg, M. (2015). Phase diagram, structures and magnetism of the $\text{FeMnP}_{1-x}\text{Si}_x$ system. *Royal Society of Chemistry*. **5**(11), 8278-8284.
- [3] Roy, P., Brück, E., & de Groot, R. A. (2016). Latent heat of the first-order magnetic transition of $\text{MnFeSi}_{0.33}\text{P}_{0.66}$. *Physical Review*. **93**(16), 165101-165111.